Surface state confinement in a lateral quantum well: The striped Cu(110)(2×1)O surface

K. Berge, A. Gerlach, G. Meister, and A. Goldmann
Fachbereich Physik, Universität Kassel, Heinrich-Plett-Strasse 40, D-34132 Kassel, Germany

E. Bertel
Institut Für Physikalische Chemie, Universität Innsbruck, Innrain 52, A-6020 Innsbruck, Austria
(Received 4 June 2004; published 5 October 2004)

We report the response of the well-known Shockley-type surface state, which resides around $\bar{Y}$ on the Cu(110) surface, to the presence of a lateral one-dimensional (1D) superlattice. This grating consists of alternating stripes of reconstructed Cu(110)(2×1)O and unreconstructed Cu(110) and can be prepared by oxygen dosing over a wide range of stripe widths and distances, respectively. Using high-resolution angle-dependent photoemission at room temperature, we study the variation of binding energy, effective mass, linewidth and energy splitting induced by the confinement perpendicular to the (2×1)O stripes. We demonstrate that the surface state electrons on the striped Cu-O surface show confinement properties and photoemission spectra in almost complete analogy to the $\bar{\Gamma}$-surface state electrons on stepped Cu(111) and Au(111) surface [Mugarza *et al.*, Phys. Rev. Lett. **87**, 107601 (2002)]. At low oxygen coverages our data differ from those of an earlier photoemission study of the same system performed with the sample at 100 K [Bertel and Lehmann, Phys. Rev. Lett. **80**, 1497 (1998)], which reports the observation of singularities in the density of states of quasi-1D subbands. However, the two studies agree within experimental error limits for the higher oxygen coverages. We explain the apparent difference by the temperature-induced transition from coherent emission out of 2D superlattice bands to incoherent emission from decoupled 1D quantum well states.

DOI: 10.1103/PhysRevB.70.155303 PACS number(s): 73.21.−b, 73.20.At, 79.60.−i

I. INTRODUCTION

The study of the electronic behavior of quantum-confined electrons is relevant in the context of fundamental condensed matter physics.[1] Moreover, since electronic and geometrical properties are connected self-consistently, any attempt to tailor electronic properties requires a deep understanding of how the electrons react to structural modifications on a nanometer scale.

Surface states on noble metals[2] have been a preferred subject of confinement-investigation in the last few years. They are accessible to scanning tunneling spectroscopy (STM) as well as to angle-resolved photoelectron spectroscopy. These methods in general yield complementary information. Photoemission can map a surface state in the reciprocal spaces of both the substrate atomic lattice and of a superlattice present at the surface in a straightforward and well-understood manner. However, it is a laterally averaging method and therefore a clear cut interpretation of the results requires regularly spaced superstructures over areas large compared to the periodicity of nanoscopic structures. In contrast, STM can resolve single terraces with defined geometry, is able to study e.g., scattering at defects and steps, and may easily identify confinement properties. While in special cases standing electron wave patterns produced by reflection at steps allowed us to map an energy versus $k_{\|}$ (momentum parallel to the surface) relation, *k*-space information regarding the superlattice is not available in general from STM.

Most studies of electron confinement in nanoscopic gratings use vicinal surfaces of noble metals. These may exhibit regularly spaced steps with experimentally tunable terrace widths in between. Strong scattering at the step edges may then lead to 1D confinement within an atomically flat terrace. In almost all cases the Shockley state around $\bar{\Gamma}$ on the noble-metal (111) surface was probed. A vicinal cut confines this surface state on (111)-oriented terraces between straight steps.[3–7] A different approach has been exploited recently by Bertel and Lehmann.[8] These authors used the quasi-one-dimensional surface oxide domains, produced[9] by self-organized stripe-pattern formation on Cu(110), to confine the Shockley-type surface state existing around $\bar{Y}$ on clean Cu(110). High-resolution angle-resolved photoemission spectra taken at $\bar{Y}$ indicate the appearance of singularities in the density of states and these are interpreted as critical points of quasi-one-dimensional subbands of the surface state electrons on the striped surface.[8] This picture appears to be in conflict with the results obtained on stepped (111)-surfaces, where around $\bar{\Gamma}$ only the ground state of the confined electrons is observed. The higher lying occupied states appear only in off-normal photoemission spectra and this may be explained quantitatively by a detailed inspection of the photoemission matrix element.[5] From an *a priori* point of view there is no clear difference between the confinement on terraces of vicinal (111) surfaces and the confinement between oxide stripes on the Cu(110)/O surface. To obtain more insight we have performed new experiments at the striped surface. The new data are taken at 300 K, while the former results[8] were obtained at 100 K. Surprisingly, the results of both experiments agree within the error bars (resulting mainly from different resolution parameters) at the higher oxygen coverages, but are different at the lower coverages. We give an interpretation for the apparent discrepancy in terms of a temperature dependent decoupling of the

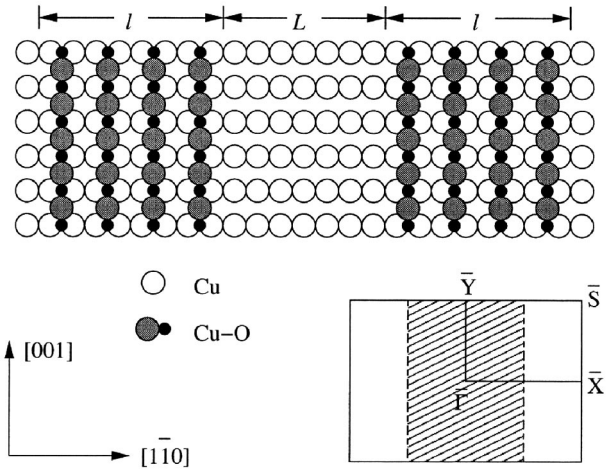

FIG. 1. Top: Atomic arrangement of the Cu-CuO stripe phase formed by alternating stripes of Cu(110) (width L) and Cu(110)(2 $\times$1)O (width l) resulting in a periodicity D=1+L of the nanograting. Note that the Cu-O chain length is large as compared to atomic distances. Bottom: crystal bulk axes (left) and surface Brillouin zone (right) for Cu(110). The dashed line shows the reduced zone (shaded) for the completely filled (2×1) overlayer configuration (L=0).

quantum well states, i.e., the transition from a coherently emitting 2D-super-lattice band structure state to emission from incoherently emitting 1D quantum-well states.

II. EXPERIMENT

The experiments were performed in an UHV system (base pressure 3×10^{-11} mbar) equipped with a hemispherical electron energy analyzer and standard facilities for sample preparation and spot-profile-analysis low-energy electron diffraction (SPALEED). The analyzer uses a channel-plate detector and an electrostatic entrance lens system which allows *in situ* variation of the angular resolution between $\Delta\theta$ $=\pm3°$ and $\pm0.4°$. The energy resolution can be tuned independent of $\Delta\theta$ by variation of the pass energy and entrance slit width. The best value of $\Delta E=12$ meV was verified by measuring the width (FWHM) of the 3*p* lines of gaseous argon after excitation with HeI ($\hbar\omega=21.2$ eV) radiation. For most spectra reported below we have chosen $\Delta\theta=\pm0.7°$ and ΔE was set between 20 and 40 meV as a compromise between resolution and intensity. All data are taken at room temperature, if not mentioned otherwise.

The sample could be rotated both with respect to the polar angle and azimuth with an accuracy of better than 0.5°. This allowed us to take spectra from extended regions of the 2D surface *k*-space, in particular, along the high-symmetry lines $\bar{\Gamma}-\bar{Y}$, $\bar{\Gamma}-\bar{X}$ and $\bar{\Gamma}-\bar{S}$; see Fig. 1 for definitions. Preparation of the Cu(110) sample consisted of repeated cycles of Ar-ion bombardment (500 eV) at 520 K and subsequent annealing at 800 K. No contamination could ever be detected with angle-resolved photoemission, and an excellent LEED pattern was observed, with a spot-width (FWHM) below 1% of the surface Brillouin zone diameter.

Adsorption was performed by the admission of molecular oxygen, with the sample at room temperature or slightly above, and subsequent annealing at 600 K. This preparation induces the quasi-1D domain structure with regularly spaced surface oxide stripes separated by stripes of clean Cu(110); see Ref. 9 for details of the preparation, and Fig. 1 for the geometry. The periodicity D could be clearly resolved using SPALEED. To determine the stripe width L, a calibration of coverage Θ_0 (defined as the ratio of the number of oxygen atoms to the number of Cu atoms in the outermost substrate layer below the Cu-O chains) is required. Our calibration results from a combined analysis of the work-function change, intensity of the oxygen-derived occupied "antibonding" UPS peak observed at $\bar{Y}$,[10,11] and the geometry parameters obtained from SPALEED, and it was corroborated a by comparison with earlier work.[8–11] The width of the clean stripes L is then given as $L=(1-\Theta_0/\Theta_s)D$, where $\Theta_s=0.5$ is the global coverage at oxygen saturation (L=0).

III. RESULTS AND DISCUSSION

A. Clean Cu(110)

To the best of our knowledge, photoemission data of the $\bar{Y}$ Shockley state have only been published along the $\bar{\Gamma}-\bar{Y}$ azimuth. Since the surface-oxide stripes also run along $\bar{\Gamma}-\bar{Y}$, confining effects are to be expected perpendicular to these stripes, i.e., along $\bar{Y}-\bar{S}$. We have therefore started our work by looking for the surface state dispersion along $\bar{Y}-\bar{S}$ and, for a comparison with earlier work, along $\bar{\Gamma}-\bar{Y}$.

Generally the surface-state dispersion with $k_\parallel$ is parabolic around the center of the surface-projected bulk band gap in which it occurs. Their photoemission initial state energy $E_i(\leqslant0$, and defined with respect to E_F at $E_i=0)$ is then described as

$$E_i = E_0(T) + \frac{\hbar^2}{2m^*}(\vec{k}_\parallel - \vec{k}_\parallel^0)^2, \tag{1}$$

where E_0 is the bottom of the parabola and $\vec{k}_\parallel^0$ gives the k-space position of the bottom, i.e., $\bar{Y}$ in the present work. The effective mass of Shockley states on the low-index noble metal surfaces is positive but generally smaller than the free-electron mass m. This indicates the essential delocalization of the surface state electrons parallel to the surface. With the sample at T=130 K we obtain $E_0=-0.47$ eV and m^*/m $=0.26\pm0.03$ along $\bar{\Gamma}-\bar{Y}$. This result is in excellent agreement with several earlier studies, see Ref. 12 and many references therein. The data of Fig. 2 show $E_0=-0.41$ eV at 300 K. From the two data points we infer a temperature dependence of E_0 with a temperature coefficient dE_0/dT $=(0.35\pm0.12)$ meV/K. This agrees within error bars with $dE_0/dT=(0.26\pm0.02)$ meV/K obtained at $\bar{Y}$ on clean Cu(110) in Ref. 12. The dispersion along $\bar{Y}-\bar{S}$ is reproduced in Fig. 2 and shows a parabola with $m^*/m=0.43\pm0.03$.

Obviously the Shockley state around $\bar{Y}$ on Cu(110) disperses anisotropically. This finding is fully supported by an

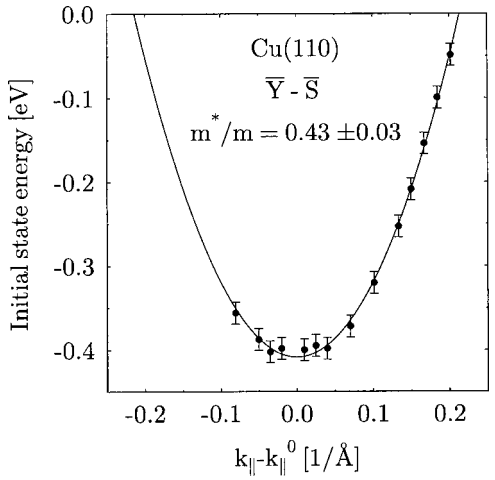

FIG. 2. Dispersion $E_i(k_\parallel)$ of the surface state around $\bar{Y}$ on Cu(110) with $k_\parallel$ running along $\bar{Y}-\bar{S}$. Photon energy $\hbar\omega=21.2$ eV; sample at 300 K. The solid line is a fit according to Eq. (1).

investigation using scanning tunneling microscopy to image the corresponding surface Fermi contour.[13] In this work the distance from $\bar{\Gamma}$ (along $\bar{\Gamma}-\bar{Y}$) to the Fermi contour is determined to be $k_F=0.68\pm0.02$ Å^{-1}, which is in excellent agreement with our result $k_F=0.67\pm0.01$ Å^{-1}. Precise data along the $\bar{Y}-\bar{S}$ direction are not given in Ref. 13. However, it is quite evident from Ref. 13 that the surface Fermi contour has elliptical shape, with the long axis along $\bar{Y}-\bar{S}$. This is clear evidence that m^* along $\bar{Y}-\bar{S}$ exceeds m^* along $\bar{\Gamma}-\bar{Y}$, in agreement with our results. The $\vec{k}$-vectors in Eq. (1) are defined with respect to the $\bar{\Gamma}$ point of the surface Brillouin zone. If we define a different 2D k-space coordinate system (k_x,k_y), with k_x along $\bar{Y}-\bar{S}$, k_y along $\bar{Y}-\bar{\Gamma}$, and $k_x=k_y=0$ just at $\bar{Y}$, we can summarize our results as

$$E_i = E_0(T) + \frac{\hbar^2}{2}\left(\frac{k_x^2}{m_x^*} + \frac{k_y^2}{m_y^*}\right), \tag{2}$$

with $m_x^*=(0.43\pm0.03)$ m and $m_y^*=(0.26\pm0.03)$ m, respectively.

A qualitative interpretation for the observed anisotropic surface state dispersion is easily presented. One reason of course is the anisotropic surface geometry with a C_{2v} point group symmetry. The physical origin of the anisotropy is given by an inspection of the origin of the Shockley state. It resides within a bulk band gap located around the $\bar{\Gamma}-\mathrm{L}$ bulk Brillouin zone direction. The projection of this gap onto the (111) surface is isotropic, and the resulting surface state appears around $\bar{\Gamma}$ on the Cu(111) surface with one effective mass of $m^*/m=0.44\pm0.03$. The surface state around $\bar{Y}$ is supported by just the same bulk band gap, which, however, is now projected onto the Cu(110) surface. In consequence, its diameter along $\bar{Y}-\bar{S}$ is identical to that on Cu(111), and the effective masses are indeed equal on Cu(111) and Cu(110). Along $\bar{Y}-\bar{\Gamma}$ the bulk gap diameter is shortened by the projection. In consequence, the surface state confined within this gap shows a narrower surface Fermi contour and a concomitant smaller effective mass. This argument is based on k-space considerations and it is instructive to complement it by investigating the surface state character in real space. The bottom of the band gap, from which the surface state is split off, is formed by an $L_{2'}$ band. This band has a pure p orbital character. The projection of these orbitals on the (110) surface and the formation of C_{2v} symmetry-adapted linear combinations yields for the surface state a p_y orbital composition.[15] Accordingly, the surface state is σ bonding in the $\bar{Y}-\bar{\Gamma}$ direction and π bonding in the $\bar{Y}-\bar{S}$ direction. Therefore, the dispersion is expected to be significantly stronger and the effective mass to be smaller in the former direction. The effect is somewhat reduced, however, by the fact that the atomic distances are larger in the $\bar{Y}-\bar{\Gamma}$ direction. By the same argument, the surface state has a p_z character and is π bonding around $\bar{\Gamma}$ on the (111) surface. With the atomic distances and the bonding type being the same as for the $\bar{Y}-\bar{S}$ direction on Cu(110) the effective masses agree to within 2%.

B. The striped Cu(110)(2×1)O surface

To determine the stripe periodicity we used SPALEED[14] to analyze electrons diffracted along $\bar{\Gamma}-\bar{X}$, i.e., the k_x direction normal to the stripes. The resulting intensity resembles very much the He-atom diffraction pattern presented in Ref. 9. It consists of the specular peak at a wave vector transfer $k_\parallel=0$, the first-order substrate peak at $k_\parallel=\pm2k_{\bar{\Gamma}\bar{X}}$ ($k_{\bar{\Gamma}\bar{X}}$ is the distance between $\bar{\Gamma}$ and $\bar{X}$), and the half-order peak at $k_\parallel=\pm k_{\bar{\Gamma}\bar{X}}$ related to the (2×1) order of the Cu-O chains on the oxygen-covered stripes. The regularly-spaced stripe-pattern gives then rise to a series of additional diffraction peaks occurring at $k_\parallel/k_{\bar{\Gamma}\bar{X}}=2\pi n/D$ with $n=\pm1,\pm2,\ldots$. These are reproduced for several coverages in Fig. 3 and allow us to determine the average stripe separation D with an accuracy of better than five percent. Combining D with the experimental oxygen coverage, the geometry parameter L and I follow immediately.

Photoelectron spectra have then been taken around $\bar{Y}$ for a striped surface with $\Theta_0=0.4$ and L=18.5 Å. Along $\bar{Y}-\bar{\Gamma}$ we observe a well-defined parabolic dispersion with an effective mass $m_y^*/m=0.26\pm0.04$, in perfect agreement with $m_y^*/m=0.26\pm0.03$ obtained from clean Cu(110). However, as to be expected, the bottom of the parabola at $\bar{Y}$ is shifted upward in initial state energy from $E_i=-0.41$ eV (clean) to -0.34 eV. Spectra measured with $k_\parallel=k_x$ along $\bar{Y}-\bar{S}$ are shown in Fig. 4 for a sample with L=19 Å. The initial state energy is $E_i=-0.35$ eV, which is accurate to ±15 meV, and the FWHM is 0.12 ± 0.01 eV at $\bar{Y}$. This result can be compared with the data obtained by Bertel and Lehmann.[8] From their spectra shown in Fig. 4 of Ref. 8, we interpolate $E_i=-0.26$ eV and a FWHM of 0.19 eV for L=19 Å. The origin of this apparent discrepancy is quite obvious: the angular acceptance is specified in Ref. 8 as $\Delta\theta=\pm2°$, as compared to ±0.7° in the present investigation. Hence, the spec-

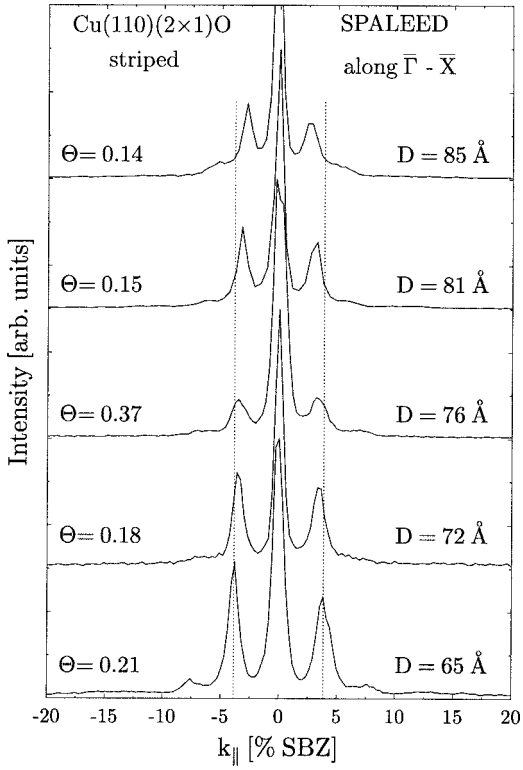

FIG. 3. Low-energy electron diffraction patterns taken from the striped Cu(110)(2×1)O surface at different oxygen coverages Θ. The wave vector $k_{\|}$ (in units of the distance $2\bar{\Gamma}\bar{X}$) is oriented perpendicular to the stripes. Sample at room temperature; electron kinetic energy 65.8 eV.

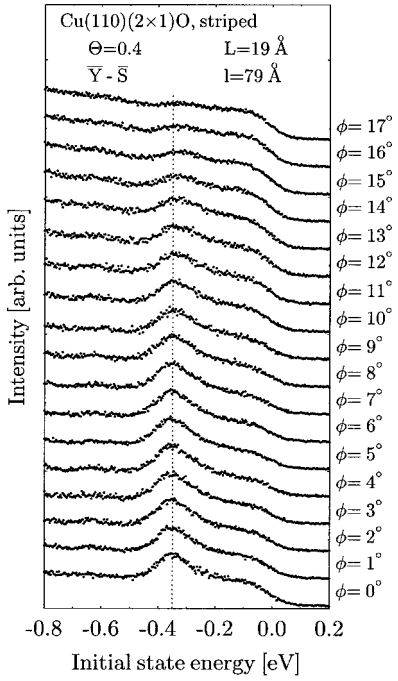

FIG. 4. (Non-)dispersion of the surface state along $\bar{Y}-\bar{S}$ between $\bar{Y}(\phi=0°)$ and $\phi=12°$, where it leaves the projected bulk band gap around $\bar{Y}$. Photon energy $\hbar\omega=21.2$ eV; angular resolution $\Delta\theta=\pm 0.7°$.

tra of Ref. 8 integrate over a larger $k_{\|}$-interval, picking up intensity from the upward dispersing branches of the surface state band. This gives rise to a larger energy broadening and also to an upward shift of the peak maximum. In addition, the channel width is determined from an independent coverage calibration using different methods in the two studies. As the quantum size shift is quite pronounced at the corresponding channel widths, a difference of only 90 meV indicates a reassuring consistency of the two studies.

To take spectra along $\bar{Y}-\bar{\Gamma}$, the sample was rotated by the polar angle θ around the manipulator axis. To detect electrons along $\bar{Y}-\bar{S}$ the sample was additionally rotated by the azimuth angle ϕ around the surface normal and the polar angle θ was increased accordingly to localize $k_{\|}$ on the $\bar{Y}-\bar{S}$ line. We indicate the experimental angle ϕ in all spectra shown in Fig. 4. The zero is chosen to meet $\bar{Y}$ at $\phi=0$.

An inspection of Fig. 4 clearly demonstrates the absence of dispersion along $\bar{Y}-\bar{S}$ up to $\phi\approx 15°$. Beyond that angle, we observe an apparent shift and simultaneously a loss of intensity. Both effects result from the fact that the surface state approaches the edge of the projected bulk band gap around $\phi\approx 16°$ and couples to the underlying bulk bands. We reach at the unique conclusion that the surface state around $\bar{Y}$ shows parabolic dispersion along $\bar{Y}-\bar{\Gamma}$, even on copper stripes as narrow as L=18.5 Å with an unchanged effective mass as compared to clean Cu(110). The absence of dispersion along $\bar{Y}-\bar{S}$ shows that the surface state is 1D as a consequence of its lateral confinement. No indication is seen in Fig. 4 for a second peak between $E_i=-0.35$ eV and the Fermi energy at $E_i=0$. If we interpret the peak at −0.35 eV as the energetic ground state of an electron confined in one dimension in a box along x, Fig. 4 indicates that the first excited state is located above E_F.

Spectra taken at an oxygen coverage of about 0.12, corresponding to copper stripes with L=73 Å, show parabolic dispersion along both the x and y directions, with effective masses equal within error bars to the results from clean Cu(110), i.e. $m_y^*=0.26$ m and $m_x^*=0.46$ m. Within the model of an electron confined in the 1D box along x, this result must be interpreted by the fact that now many levels contribute. Their spacing is so small that they cannot be resolved individually. Moreover, however, the parabolic dispersion along k_x gives clear evidence that the photoexcitation matrix element is strongly dependent on k_x. Obviously at $k_x=k_y=0$ only the ground state of the electron in the box is observed. With increasing k_x (and $k_y=0$) the higher-lying box states are subsequently contributing to the photocurrent. This then mimics a parabolic dispersion.

Figure 5 reproduces data taken along $\bar{Y}-\bar{S}$ from a sample with L=32 Å. At $\bar{Y}$ ($\phi=0°$) we resolve one peak at $E_i=-0.38$ eV. With increasing rotation angle ϕ, i.e., with increasing distance from $\bar{Y}$, a second peak around $E_i=-0.15$ eV gains intensity. It survives longer than the peak at −0.38 eV, until finally near $\phi=17°$ the edge of the underlying bulk band gap is approached and both lose intensity rapidly. We note that no dispersion is resolved within our

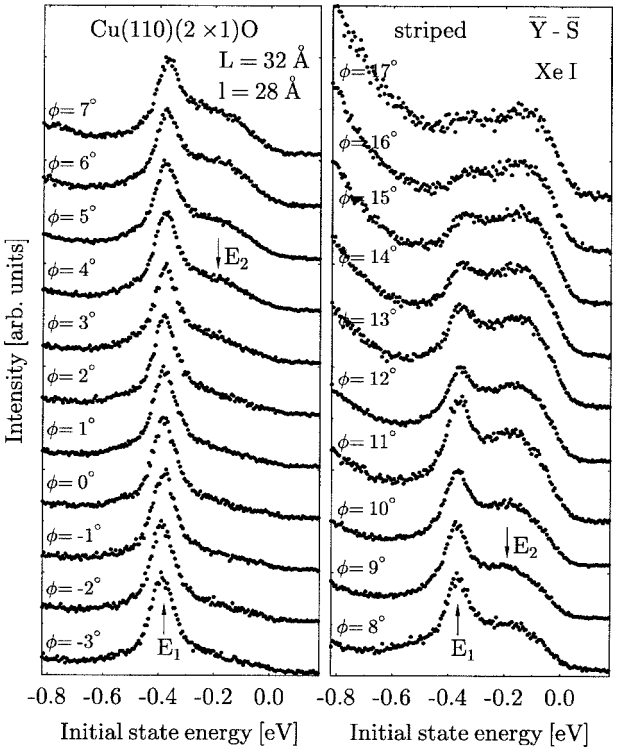

FIG. 5. Surface state spectra taken along $\bar{Y}-\bar{S}$ from a surface with L=32 Å. Note that intensities are not drawn to scale, but are exaggerated for higher azimuthal angles ϕ to make weak features better visible. Photon energy $\hbar\omega$=8.3 eV (Xe I).

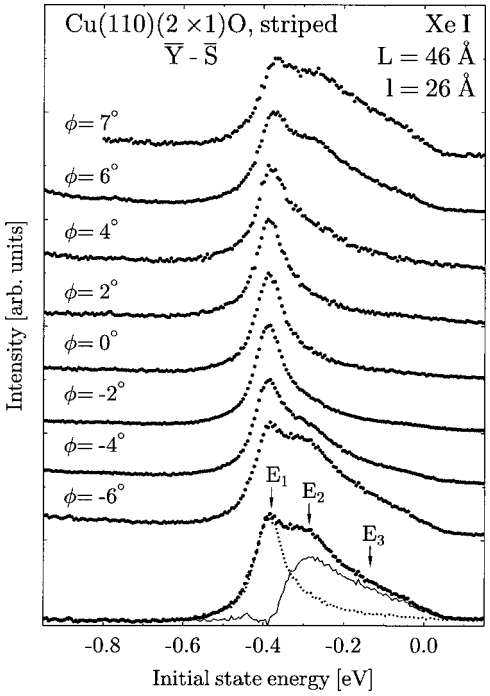

FIG. 6. The same Fig. 5, but for a sample with L=46 Å. The bottom curves show the difference spectrum obtained by subtracting the ϕ=0° spectrum from the ϕ=−6° spectrum after appropriate normalization of intensities at E_i=−0.4 eV.

accuracy. Data taken along $\bar{Y}-\bar{\Gamma}$ reveal a well-defined parabolic dispersion with m^*=0.26 m in agreement with our results on clean Cu(110). Finally, we present results along $\bar{Y}-\bar{S}$ for L=46 Å in Fig. 6. Now again we resolve one clear peak at E_i=−0.39 eV around ϕ=0° i.e., at $\bar{Y}$. A second and third peak develop intensity with increasing ϕ at initial state energies around −0.28 and 0.11 eV, respectively. Also in this case the parabolic dispersion along the Cu stripes is equal to that obtained for the clean sample.

We summarize our experimental results as follows. Along $\bar{Y}-\bar{\Gamma}$ the dispersion is the same for all geometries between L=18.5 Å and $L\rightarrow\infty$ with m_y^*=(0.26±0.03) m and the energy dependence $\hbar^2k_y^2/(2m_y^*)$. However, due to the lateral confinement along x($\bar{Y}-\bar{S}$), the bottom of this parabola shifts upward to E_F. The corresponding energy values are summarized in Fig. 7(a). We observe 1D behavior for 18.5 Å$\lesssim L\lesssim$60 Å, with additional quantum levels resolved between $L\approx$30 Å and 50 Å. Only the ground state (n=1) is observed with significant photoemission intensity at k_x=0, k_y=0. With increasing k_x the second (n=2) and third (n=3) quantum-well states appear in the spectra. We did not analyze their intensity in detail, since in our experimental arrangement a light incidence angle (and therefore the degree of light polarization) and k_x vary simultaneously, and this makes any interpretation of intensity versus k_x uncertain. Following Eq. (2), the surface states on the striped surface with 18.5 Å$\lesssim L\lesssim$60 Å may be described as

$$E_i = E_0(T) + \left(E_n(L) + \frac{\hbar^2 k_y^2}{2m_y^*}\right), \tag{3}$$

where $E_n(L)$ represents the 1D quantized states (n=1,2,3,…) on a Cu stripe of width L.

The Shockley state on the striped Cu(110)/O surface has been studied already in Ref. 8. Photoemission spectra taken just at $\bar{Y}$ show, besides the expected peak from the bottom (k_x=k_y=0) of the surface state parabola, additional narrow features on the low binding energy side of the surface state peak. These are clearly resolved for coverages between 0.13 (L=54 Å) and 0.22 (L=38 Å). In the spectrum obtained at L=48 Å (Θ_0=0.16) the additional peaks are located at E_i=−0.34 eV, −0.23 eV and (with less certainty) at −0.11 eV. At Θ=0.19 (L=42 Å) all peaks are slightly upward shifted. None of these peaks has ever been detected in our present study at $\bar{Y}$, although we started a careful search, with different photon energies between $\hbar\omega$=8.3 eV and 21.2 eV. On the other hand, our results like those presented in Figs. 2–6 were safely reproduced with different photon energies and after various sample preparations. The data from Ref. 8 were taken at T=100 K, where the experimental width at the bottom of the parabola on clean Cu(110) is below 70 meV,[12] while an experimental FWHM of 126 meV was resolved in Ref. 8. Our data were taken at T=300 K, where we resolved a FWHM of 82 meV on clean Cu(110), in perfect agreement with 86 meV observed in an earlier high-resolution study.[12] How can we explain the apparent discrepancy? The additional peaks reported in Ref. 8 appear

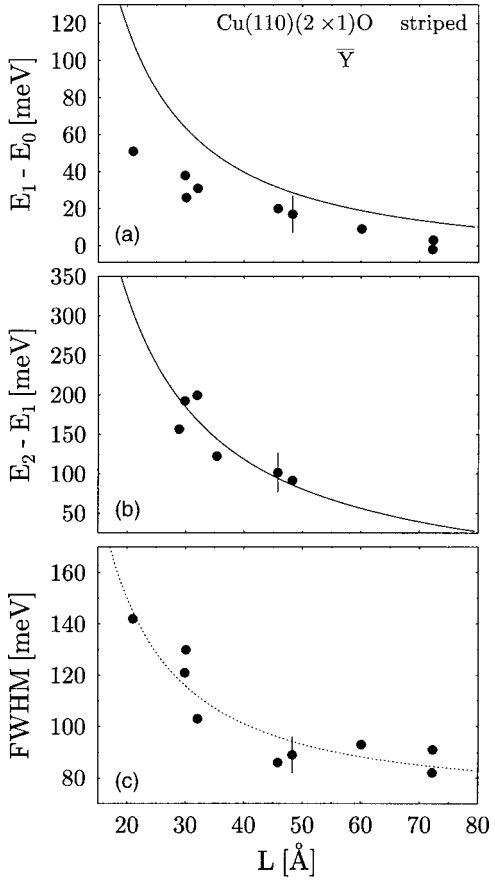

FIG. 7. (a) Energy shift $E_1(\mathrm{L})-E_0$ as a function of stripe width L, compare with Eq. (3) for a definition. Experimental data points are compared to result of the Kronig-Penney model (solid line) calculated with $V_0=0.7$ eV. (b) Energy difference E_2-E_1 in its dependence on L (data points) and a result of the Kronig-Penney model calculation (solid line, $V_0=0.7$ eV). (c) Experimental FWHM of the surface state peak at $\bar{\mathrm{Y}}$ as a function of L.

at almost the same initial state energies as the quantum-well states observed in our study at $|k_x|>0$. Hence, the features could have been detected under the experimental conditions of Ref. 8, if there was a sample misalignment by about 3° (rotation about the $\bar{\Gamma}-\bar{\mathrm{Y}}$ axis). This possibility, however, can be ruled out. An examination of LEED photographs taken during the earlier study[8] safely exclude a misalignment exceeding 1°. Furthermore, the structures detected in Ref. 8 were more distinct than those seen in the present study, despite the lower resolution in the previous experiment. This clearly hints toward a different mechanism giving rise to the photoemission features. We remain with the conclusion that the differences between the results from Ref. 8 and the present work must result from the different sample temperatures. We come back to this point later.

The quantum-well states show no dispersion along k_x within the error bars. This indicates almost complete confinement and only weak coupling between adjacent Cu stripes. Such a situation was also reported for the Shockley state around $\bar{\Gamma}$ on Au(111) terraces of the vicinal Au(788) surface.[5] On the stepped Au(111) surface the energy spacing between E_2 and E_1 [compare Eq. (3) for a definition] could

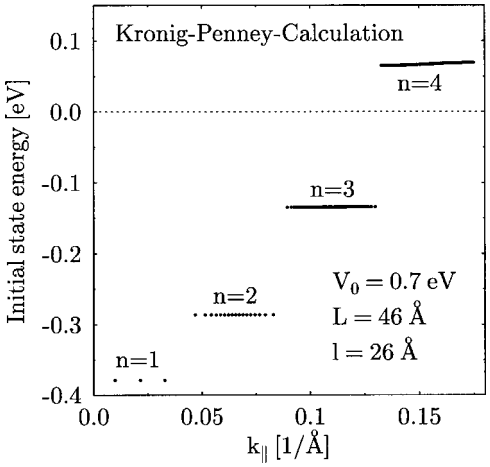

FIG. 8. Energy eigenvalues calculated from the 1D Kronig-Penney model with a well depth of $V_0=0.7$ eV. The geometry parameters L and l correspond to Fig. 6.

be explained quantitatively by the energy eigenvalues of the infinite 1D quantum well of size L, where

$$E_n=\frac{\hbar^2\pi^2}{2m^*L^2}n^2, \tag{4}$$

and m^* is the effective mass observed on the flat Au(111) surface. This formula fails to explain our data, giving too large energy spacings. Obviously the electron wave function extends considerably into the quantum barrier created by the Cu−O stripes. To obtain a more realistic description we have therefore made some calculations using the Kronig-Penney model, consisting of a 1D periodic array of rectangular potential wells of width L and barriers of width l and finite height V_0. L and l are taken from the experiment, the interaction of the surface state electron with the substrate is summarized by using the experimental parameters E_0 and m_x^*, see Eq. (3) for a definition. Therefore only V_0 can be adjusted to the experiment as a free parameter. As suggested already in Ref. 8 an upper limit for the well depth V_0 can be derived from the difference of the $\bar{\mathrm{Y}}$-surface-state position on clean Cu(110) and on the oxygen-saturated Cu(110)(2×1)O surface. This estimate yields $V_0=1.1$ eV. A lower limit results from the difference in the work function between the two surfaces, giving $V_0=0.4$ eV. We have therefore chosen $V_0=0.7$ eV as a compromise and with this parameter we obtain a reasonable overall description of our experimental results. Indeed one should not expect that V_0 is constant for 1D levels confined in a box of variable width L: At large L, the surface state lies rather close to the bottom of the projected bulk band gap. With decreasing L the surface state shifts upward, thereby the spatial extension into the bulk changes, and the influence of the confining oxide potential varies continuously.

A typical result, showing the calculated 1D states in an extended zone scheme, is reproduced in Fig. 8. These levels correspond to those observed in Fig. 6. The calculated shift of the n=1 state is $E_1-E_0=0.03$ eV, somewhat larger than the experimental value of 0.02 eV. A smaller value of V_0

would improve the agreement. However, the calculated energy splitting $E_2-E_1=0.09$ eV is in good agreement with the experimental $E_2-E_1=0.10$ eV. Also, the theoretical value $E_3-E_2=0.15$ eV (E_3 is indicated in Fig. 6 by an arrow) is consistent with the experiment. Calculated and experimental data obtained for other values of L are shown in Figs. 7(a) and 7(b). Given the fact that a Kronig-Penney-type rectangular potential with depth V_0 is a severe simplification, we can state that the calculations describe all experimental trends quite well.

We have also analyzed the linewidth Γ (FWHM) of the n=1 peak at $\bar{Y}$ in its dependence on L. The results are summarized in Fig. 7(c). For $L\rightarrow\infty$ we obtain $\Gamma=87$ meV at 300 K, in excellent agreement with earlier data.[12] At $L<40$ Å the width Γ increases, by up to a factor 1.6 at L =21 Å. This effect may be explained quantitatively if we consider that L is not constant everywhere but may vary by one chain distance $\pm\Delta L=5.1$ Å. The concomitant shift of E_1, leads to the broadening by integration over regions with different L. Therefore our data give no hint that the observed broadening could be due to L-dependent lifetime effects of the photohole.

Finally, we have to explain why at $\bar{Y}$ only the E_1 peak is observed. E_2 and E_3 are seen with significant intensity only along $\bar{Y}-\bar{S}$, i.e., at $(k_y=0, k_x>0)$. An interpretation for the analogous effect observed for laterally confined states on stepped Au(111) has been presented recently by Mugarza *et al.*[5] These authors have made an estimate of the photoemission matrix element and the corresponding intensity $I(k_x)$. They show that $I(k_x)$ essentially describes the probability density $|\psi(k_x)|^2$ of the confined electron wave function ψ in reciprocal space. For the limiting case of $V_0\rightarrow\infty$, i.e., the infinite 1D quantum well of size L, ψ is known and one can derive a formula for $I(k_x)$. If we apply this formula to our experiment at L=32 Å, the E_2 state is predicted to be intense between about $\phi=5.5°$ ($k_x=0.08$ Å^{-1}) and $\phi=16°$ ($k_x=0.25$ Å^{-1}). An inspection of Fig. 6 shows surprisingly good agreement with the experiment. Similar agreement is found for other values of L. We remind the reader that this model assumes ($V_0\rightarrow\infty$) a complete decoupling of the individual quantum well states, i.e., an incoherent contribution of each confined (1D) surface state to the observed photoemission intensity. On the other hand, we have seen that the Kronig-Penney model describes the data better than the isolated-quantum-well model. Apparently the physical situation exhibits traits of both. In other words, this seems to be a case where the surface state wave function is just at the transition between a two-dimensional Bloch state in the superlattice and an ensemble of one-dimensional, decoupled quantum well states. In the former case, the angle dependence of the photoemission yield is governed by the extension of the SBZ of the superlattice, as discussed in Ref. 8. In the latter case, the analysis of Mugarza *et al.*[5] applies, yielding the results observed in the present study. In principle, the balance can be tipped in favor of the 1D case by two different effects: first, a slight disorder with regard to the channel width could give rise to a 1D localization. However, considering the LEED pattern obtained in the present study (see Fig. 3), we conclude that the stripe pattern was at least as well developed as in the previous work. Second, temperature is an important parameter in such borderline situations. The coupling energy t across the oxide stripes is obviously weak, and if kT becomes comparable to t, a breakdown of the coherent coupling has to be expected. Given the fact that the measuring temperature in the present study was three times as high as in Ref. 8, it is actually not surprising that the present data indicate incoherent emission from 1D states, whereas coherent emission from a 2D state was observed in Ref. 8. The higher features reported in Ref. 8 are observable at $\bar{Y}$ only due to coherent scattering (Umklapp) processes. Obviously, if the phase coherence is destroyed, Umklapps lose their significance and the corresponding features at $\bar{Y}$ disappear.

In conclusion, the assumption of a temperature-dependent decoupling of the quantum well states is consistent with all observations reported so far. It indicates that kT is of the order of the coupling energy t at about 300 K. Also, for the higher oxygen coverages the two studies of the striped Cu(110)/O surface agree to within experimental error limits. For this case the presence of incoherent 1D quantum well states is concluded already at 100 K. Thus, the present data indicate that the striped O/Cu(110) surface is a comparatively simple model system, where temperature-induced coherent-incoherent transitions can be studied without complications, arising from insufficient control over structure and chemical composition, which generally mar measurements in more complex systems. Such studies are of general relevance, as coherent-incoherent transitions occur in a wide variety of technologically important materials ranging from Kondo systems to high-temperature superconductors.

ACKNOWLEDGMENTS

Our work in Kassel has been continuously supported by the Deutsche Forschungsgemeinschaft (DFG), the work in Innsbruck by the Austrian Science Fund (FWF).

[1] M. F. Crommie, C. P. Lutz, and D. M. Eigler, Nature (London) **363**, 524 (1993); **369**, 464 (1994).

[2] *Electronic Surface and Interface States on Metallic Systems*, edited by E. Bertel and M. Donath (World Scientific, Singapore, 1995).

[3] J. E. Ortega, S. Speller, A. R. Bachmann, A. Mascaraque, E. G. Michel, A. Närmann, A. Mugarza, A. Rubio, and F. J. Himpsel, Phys. Rev. Lett. **84**, 6110 (2000).

[4] F. Baumberger, T. Greber, and J. Osterwalder, Phys. Rev. B **62**, 15431 (2000).

[5] A. Mugarza, A. Mascaraque, V. Pérez-Dieste, V. Repain, S. Rousset, F. J. García de Abajo, and J. E. Ortega, Phys. Rev. Lett. **87**,

107601 (2001).
[6] X. J. Shen, H. Kwak, D. Mocuta, A. M. Radojevic, S. Smadici, and R. M. Osgood, Jr., Phys. Rev. B **63**, 165403 (2001).
[7] A. Mugarza, A. Mascaraque, V. Repain, S. Rousset, K. N. Altmann, F. J. Himpsel, Yu. M. Koroteev, E. V. Chulkov, F. J. Garcia de Abajo, and J. E. Ortega, Phys. Rev. B **66**, 245419 (2002).
[8] E. Bertel and J. Lehmann, Phys. Rev. Lett. **80**, 1497 (1998).
[9] K. Kern, H. Niehus, A. Schatz, P. Zeppenfeld, J. Goerge, and G. Comsa, Phys. Rev. Lett. **67**, 855 (1991).
[10] R. Courths, S. Hüfner, P. Kemkes, and G. Wiesen, Surf. Sci. **376**, 43 (1997).
[11] F. Pforte, A. Gerlach, A. Goldmann, R. Matzdorf, J. Braun, and A. Postnikov, Phys. Rev. B **63**, 165405 (2001).
[12] P. Straube, F. Pforte, T. Michalke, K. Berge, A. Gerlach, and A. Goldmann, Phys. Rev. B **61**, 14072 (2000).
[13] L. Petersen, B. Schaefer, E. Lægsgaard, I. Stensgard, and F. Besenbacher, Surf. Sci. **457**, 319 (2000).
[14] M. Henzler, in *The Structure of Surfaces*, edited by M. A. van Hove and J. F. Van der Veen, Springer Series in Surface Science Vol. 11 (Springer-Verlag, Berlin, 1988).
[15] E. Bertel, Phys. Rev. B **50**, 4925 (1994).